

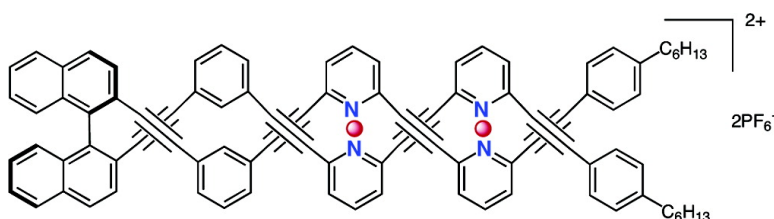
Article

Metal-Assisted Assembly of Pyridine-Containing Arylene Ethynylene Strands to Enantiopure Double Helicates

Akihiro Orita, Takehiro Nakano, De Lie An, Kazumi Tanikawa, Kan Wakamatsu, and Junzo Otera

J. Am. Chem. Soc., **2004**, 126 (33), 10389-10396 • DOI: 10.1021/ja048327d • Publication Date (Web): 30 July 2004

Downloaded from <http://pubs.acs.org> on April 1, 2009



More About This Article

Additional resources and features associated with this article are available within the HTML version:

- Supporting Information
- Links to the 6 articles that cite this article, as of the time of this article download
- Access to high resolution figures
- Links to articles and content related to this article
- Copyright permission to reproduce figures and/or text from this article

[View the Full Text HTML](#)



ACS Publications
 High quality. High impact.

Metal-Assisted Assembly of Pyridine-Containing Arylene Ethynylene Strands to Enantiopure Double Helicates

Akihiro Orita,[†] Takehiro Nakano,[†] De Lie An,[†] Kazumi Tanikawa,[†]
Kan Wakamatsu,[‡] and Junzo Otera^{*†}

Contribution from the Departments of Applied Chemistry and Chemistry,
Okayama University of Science, Ridai-cho, Okayama 700-0005, Japan

Received March 23, 2004; E-mail: otera@high.ous.ac.jp

Abstract: Pyridine-containing arylene ethynylene strands were connected to the 2- and 2'-positions of (*R*)- and (*S*)-1,1'-binaphthyl templates. The arylene ethynylene moieties underwent intramolecular coordination with Ag(I) or Cu(I) ion to afford enantiopure double helicates. The double-helical structure was elucidated on the basis of circular dichroic (CD) spectra. The importance of intramolecular complexation of the double strands for the helicate formation was confirmed by comparison with a ligand bearing a single strand. Connection of the strands through an ether linkage enabled a sorting out of the Cotton effect induced by double-helical arylene ethynylene moieties. The CD exciton chirality method unambiguously proved that the termini of the strands approach each other upon complexation and that the sense of the induced helicity is the same as predicted by molecular modeling.

Introduction

Extensive attention has been paid to the self-assembly of double helicates, some now available even in enantiomerically pure form.¹ Metal coordination chemistry has played a pivotal role for this purpose since the pioneering work by Lehn et al.² The most common way to arrive at homochiral helicates is to introduce a chiral center into the backbone of the ligand strand.³ Spontaneous resolution is also effective on some occasions.⁴ Another strategy is to attach ligand strands to a chiral template as developed by Cozzi and Siegel and co-workers.⁵ During a project on arylene ethynylene chemistry, we reported the synthesis of an enantiopure double-helical phenylene ethynylene cyclophane.⁶ Consequently, we have become interested in acyclic analogues because no such motif is known, in contrast to extensive work on the relevant single helices.⁷ Inspection of molecular models suggested to us that the double-helix arrangement would be feasible if the strands with alternating ethynylene/*meta*-arylene arrays were connected to the 2- and 2'-positions of a 1,1'-binaphthalene template. However, preliminary experiments soon revealed that no helical structures could be attained by use of simple phenylene ethynylene chains due to the lack of effective interactions between them. We were then intrigued

by the Cozzi/Siegel strategy. On the basis of molecular modeling, pyridine was found to be a suitable donor unit due

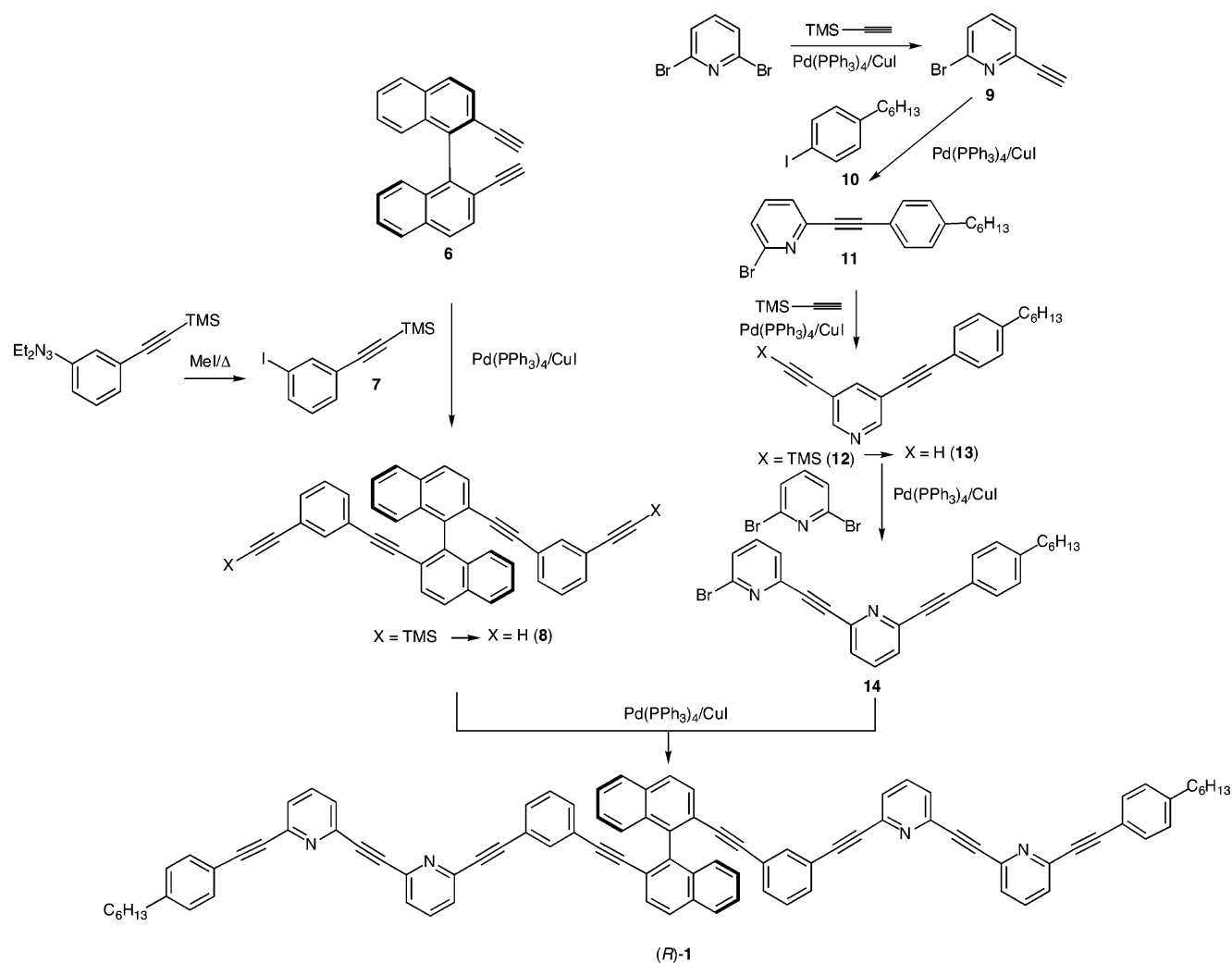
[†] Department of Applied Chemistry.

[‡] Department of Chemistry.

- (1) For some representative reviews: (a) Lehn, J.-M. *Supramolecular Chemistry*, VCH: Weinheim, Germany, 1995. (b) Lehn, J.-M. *Angew. Chem., Int. Ed. Engl.* **1988**, *27*, 89–112. (c) Lehn, J.-M. *Angew. Chem., Int. Ed. Engl.* **1990**, *29*, 1304–1319. (d) Lindsey, J. S. *New J. Chem.* **1991**, *15*, 153–180. (e) Constable, E. C. *Tetrahedron* **1992**, *48*, 10013–10059. (f) Piguet, C.; Bernardinelli, G.; Hopfgartner, G. *Chem. Rev.* **1997**, *97*, 2005–2062. (g) Albrecht, M. *Chem. Soc. Rev.* **1998**, *27*, 281–287. (h) Albrecht, M. *Chem. Eur. J.* **2000**, *6*, 3485–3489. (i) Holliday, B. J.; Mirkin, C. A. *Angew. Chem., Int. Ed.* **2001**, *40*, 2022–2043. (j) Hill, D. J.; Mio, M. J.; Prince, R. B.; Hughes, T. S.; Moore, J. S. *Chem. Rev.* **2001**, *101*, 3893–4011.
- (2) Lehn, J.-M.; Rigault, A.; Siegel, J. S.; Harrowfield, J.; Chevrier, B.; Moras, D. *Proc. Natl. Acad. Sci. U.S.A.* **1987**, *84*, 2565–2569.

- (3) (a) Libman, J.; Tor, Y.; Shanzer, A. *J. Am. Chem. Soc.* **1987**, *109*, 5880–5881. (b) Shanzer, A.; Libman, J.; Lifson, S. *Pure Appl. Chem.* **1992**, *64*, 1421–1435. (c) Koert, U.; Harding, M. M.; Lehn, J.-M. *Nature* **1990**, *346*, 339–342. (d) Zarges, W.; Hall, J.; Lehn, J.-M.; Bolm, C. *Helv. Chim. Acta* **1991**, *74*, 1843–1852. (e) Enemark, E. J.; Stack, T. D. P. *Angew. Chem., Int. Ed. Engl.* **1995**, *34*, 996–998. (f) Constable, E. C.; Kulke, T.; Neuberger, M.; Zehnder, M. *Chem. Commun.* **1997**, 489–490. (g) Baum, G.; Constable, E. C.; Fenske, D.; Kulke, T. *Chem. Commun.* **1997**, 2043–2044. (h) Baum, G.; Constable, E. C.; Fenske, D.; Housecroft, C. E.; Kulke, T. *Chem. Commun.* **1998**, 2659–2660. (i) Baum, G.; Constable, E. C.; Fenske, D.; Housecroft, C. E.; Kulke, T. *Chem. Eur. J.* **1999**, *5*, 1862–1873. (j) Baum, G.; Constable, E. C.; Fenske, D.; Housecroft, C. E.; Kulke, T.; Neuberger, M.; Zehnder, M. *J. Chem. Soc., Dalton Trans.* **2000**, 945–959. (k) Bowyer, P. K.; Porter, K. A.; Rae, A. D.; Willis, A. C.; Wild, S. B. *Chem. Commun.* **1998**, 1153–1154. (l) Mürner, H.; von Zelewsky, A.; Hopfgartner, G. *Inorg. Chim. Acta* **1998**, *271*, 36–39. (m) Mamula, O.; von Zelewsky, A.; Bernardinelli, G. *Angew. Chem., Int. Ed.* **1998**, *37*, 290–293. (n) Mamula, O.; von Zelewsky, A.; Bark, T.; Bernardinelli, G. *Angew. Chem., Int. Ed.* **1999**, *38*, 2945–2948. (o) Mamula, O.; Monlien, F. J.; Porquet, A.; Hopfgartner, G.; Merbach, A. E.; von Zelewsky, A. *Chem. Eur. J.* **2001**, *7*, 533–539. (p) Muller, G.; Bünzli, J.-C. G.; Riehl, J. P.; Suhr, D.; von Zelewsky, A.; Mürner, H. *Chem. Commun.* **2002**, 1522–1523.
- (4) (a) Krämer, R.; Lehn, J.-M.; De Cian, A.; Fischer, J. *Angew. Chem., Int. Ed. Engl.* **1993**, *32*, 703–706. (b) Kersting, B.; Meyer, M.; Powers, R. E.; Raymond, K. N. *J. Am. Chem. Soc.* **1996**, *118*, 7221–7222.
- (5) (a) Woods, C. R.; Benaglia, M.; Cozzi, F.; Siegel, J. S. *Angew. Chem., Int. Ed. Engl.* **1996**, *35*, 1830–1833. (b) Annunziata, A.; Benaglia, M.; Cinquini, M.; Cozzi, F.; Woods, C. R.; Siegel, J. S. *Eur. J. Org. Chem.* **2001**, 173–180.
- (6) (a) An, D. L.; Nakano, T.; Orita, A.; Otera, J. *Angew. Chem., Int. Ed.* **2002**, *41*, 171–173. (b) Orita, A.; An, D. L.; Nakano, T.; Yaruva, J.; Ma, N.; Otera, J. *Chem. Eur. J.* **2002**, *8*, 2005–2010.
- (7) For the most recent papers: (a) Cary, J. M.; Moore, J. S. *Org. Lett.* **2002**, *4*, 4663–4666. (b) Matsuda, K.; Stone, M. T.; Moore, J. S. *J. Am. Chem. Soc.* **2002**, *124*, 11836–11837. (c) Zhao, D.; Moore, J. S. *J. Am. Chem. Soc.* **2002**, *124*, 9996–9997. (d) Kübel, C.; Mio, M. J.; Moore, J. S. *J. Am. Chem. Soc.* **2002**, *124*, 8605–8610. (e) Nishinaga, T.; Tanatani, A.; Oh, K.; Moore, J. S. *J. Am. Chem. Soc.* **2002**, *124*, 5934–5935. (f) Zhao, D.; Moore, J. S. *J. Org. Chem.* **2002**, *67*, 3548–3554. (g) Tanatani, A.; Hughes, T. S.; Moore, J. S. *Angew. Chem., Int. Ed.* **2002**, *41*, 325–328. (h) Ma, L.; Hu, Q.-S.; Vitthana, D.; Wu, C.; Kwan, C. M. S.; Pu, L. *Macromolecules* **1997**, *30*, 204–218. (i) Lère-Porte, J.-P.; Moreau, J. J. E.; Serein-Spiran, F.; Nakim, S. *Chem. Commun.* **2002**, 3020–3021. (j) Prince, R. B.; Okada, T.; Moore, J. S. *Angew. Chem., Int. Ed.* **1999**, *38*, 233–236.

Scheme 1



to fitness of the metal–nitrogen coordination bond in the rigid arylene ethynylene double-helical systems.⁸ The binaphthyl group was a stereogenic template of choice because of its facile availability.⁹ Herein we report that the pyridine-containing arylene ethynylene strands can be assembled through metal coordination to form novel enantiopure double helicates.

Results and Discussion

After screening a variety of arrays of the benzene and pyridine rings in the strand, we concluded that intervention of two pyridine rings gave rise to the most effective complexation. One pyridine ring in each strand is not sufficient to induce effective metal complexation, while three pyridines result in insoluble complexes. The synthetic procedure for the requisite substrate (R)-1 is shown in Scheme 1. The *n*-hexyl groups attached to the terminal benzene rings are necessary to impart better solubility. First, direct Sonogashira coupling between 6 and the

required residues containing four aromatic rings was attempted but failed, probably because of the steric congestion of the reaction sites in 6. Accordingly, this template was converted to 8 by reaction with more reactive 7. The Sonogashira coupling of this intermediate with 14 smoothly took place to afford a reasonable yield of (R)-1. The enantiomer (S)-1 was obtained analogously. The structures of the compounds were fully confirmed by elemental analysis, mass spectrometry, and NMR spectroscopy (Figure 1a).

Metal complexation was straightforward. To a tetrahydrofuran (THF) solution of either (R)- or (S)-1 (1 equiv) was added a THF solution of AgPF₆ (2.2 equiv) in the dark at room temperature (Scheme 2). The complex 2a precipitated immediately as a white solid. The ¹H NMR spectrum of 2a revealed that H_a and H_c experienced an appreciable upfield shift relative to 1, while the H_b resonance was shifted downfield (Figure 1b). In the complex, H_a and H_c are situated in the diamagnetic region of the binaphthyl group, and H_b is deshielded by a phenyl ring of the counterpart strand. These shifts suggest that the freely moving strands in 1 are immobilized as in 2a. The corresponding copper(I) complexes 2b were obtained analogously as yellow precipitates when (R)- or (S)-1 was added to [(CH₃CN)₄Cu]PF₆ (2.2 equiv) in CH₂Cl₂. NMR spectra of

(8) Metal complexes with linear ethynylpyridines: (a) Potts, K. T.; Horwitz, C. P.; Fessak, A.; Keshavarz-K, M.; Nash, K. E.; Toscano, P. J. *J. Am. Chem. Soc.* **1993**, *115*, 10444–10445. (b) Sun, S.-S.; Lees, A. *J. Am. Chem. Soc.* **2000**, *122*, 8956–8967. (c) Kawano, T.; Kuwana, J.; Shinomaru, T.; Du, C.-X.; Ueda, I. *Chem. Lett.* **2001**, 1230–1231. (d) Kawano, T.; Shinomaru, T.; Ueda, I. *Org. Lett.* **2002**, *4*, 2545–2547. (e) Kawano, T.; Kato, T.; Du, C.-X.; Ueda, I. *Bull. Chem. Soc. Jpn.* **2003**, *76*, 709–719. (f) Kawano, T.; Kuwana, J.; Ueda, I. *Bull. Chem. Soc. Jpn.* **2003**, *76*, 789–797. (g) Tomozaki, K.-y.; Yu, L.; Wei, L.; Lindsey, J. S. *J. Org. Chem.* **2003**, *68*, 8199–8207. (h) Chi, K.-W.; Addicott, C.; Arif, A. M.; Das, N.; Stang, P. J. *J. Org. Chem.* **2003**, *68*, 9798–9801.

(9) For the use of binaphthyl derivatives as stereogenic core, see Pu, L. *Chem. Rev.* **1998**, *98*, 2405–2494.

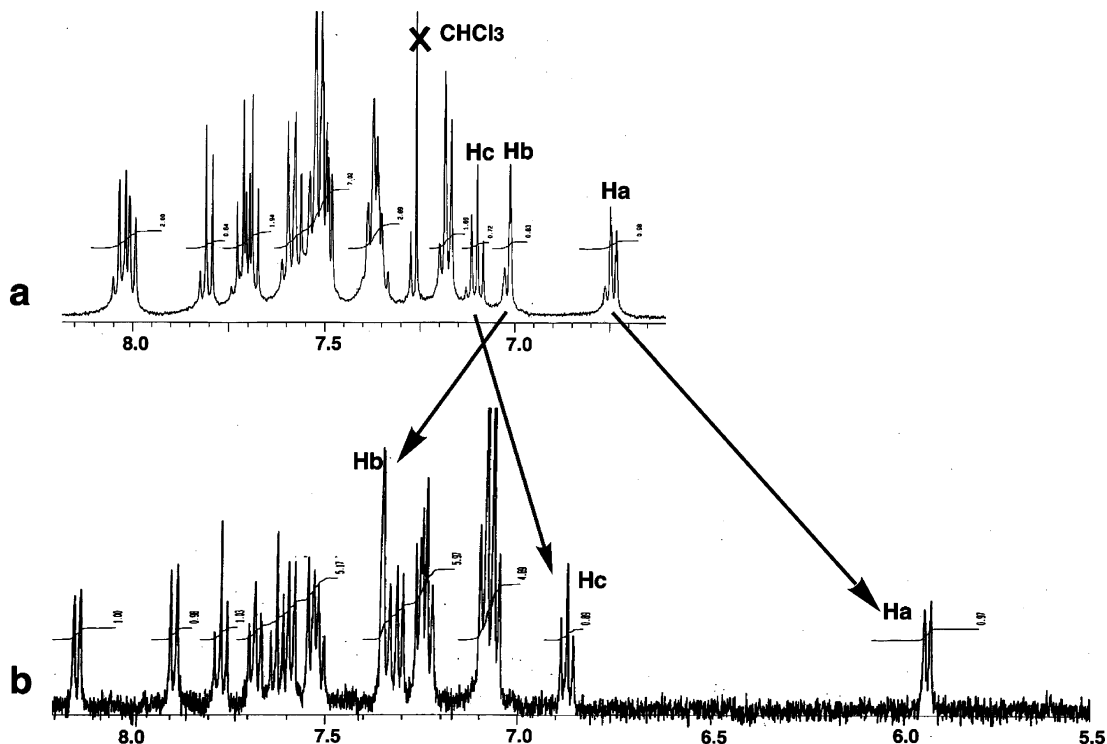
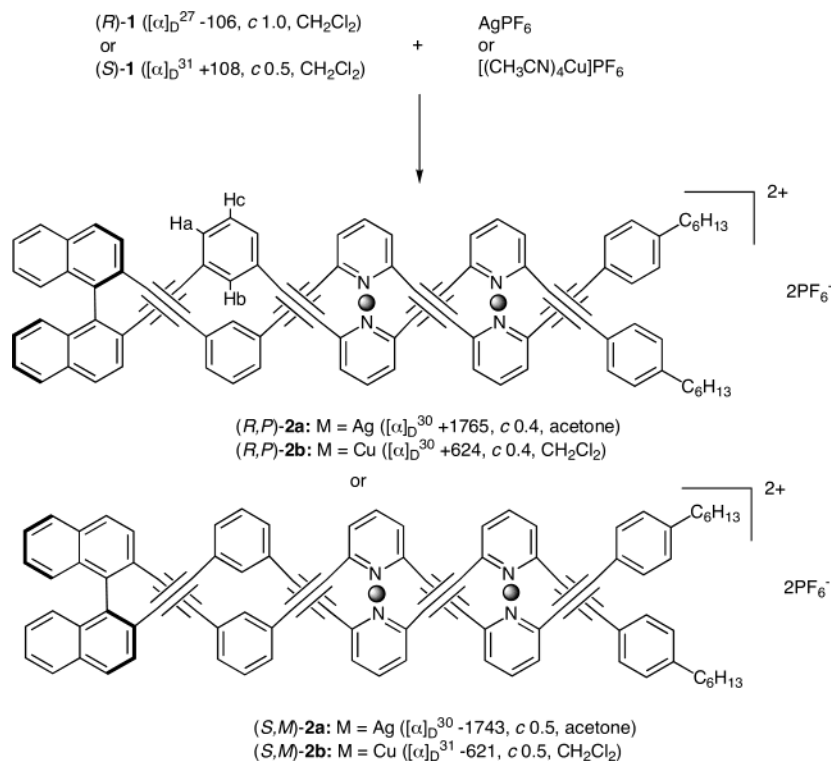


Figure 1. ^1H NMR spectra of **1** and **2a**: (a) **1** in CDCl_3 ; (b) **2a** in $\text{acetone-}d_6$.

Scheme 2



these complexes exhibited slightly broad signals, possibly due to dynamic dissociation. Such slight instability may be ascribed to the two-coordinate metal complex.¹⁰ Some two-coordinate Cu(I) and Ag(I) complexes are known,^{3f,11} and a dynamic change of bonding mode was suggested for Cu(I)^{11b} and Ag(I)^{11e}

(10) Metal coordination with the acetylene moiety is not plausible because no complexes were formed with phenylene/ethynylene analogues without pyridine spacers. ^{13}C NMR spectra also did not indicate such interactions.

complexes. Confirmation of the 2:1 metal/**1** stoichiometry of complexes **2a** and **2b** was attempted by electrospray and matrix-assisted laser desorption ionization time-of-flight (MALDI-TOF) mass spectrometries. However, both methods gave rise to no

(11) (a) Sorrel, T. N.; Borovik, A. S. *J. Am. Chem. Soc.* **1986**, *108*, 5636–5637. (b) Piguat, C.; Bernardinelli, G.; Williams, A. F. *Inorg. Chem.* **1989**, *28*, 2920–2925. (c) Rüttimann, S.; Piguat, C.; Bernardinelli, G.; Bocquet, B.; Williams, A. F. *J. Am. Chem. Soc.* **1992**, *114*, 4230–4237. (d) Cardina, R.; Williams, A. F.; Piguat, C. *Helv. Chim. Acta* **1998**, *81*, 548–557.

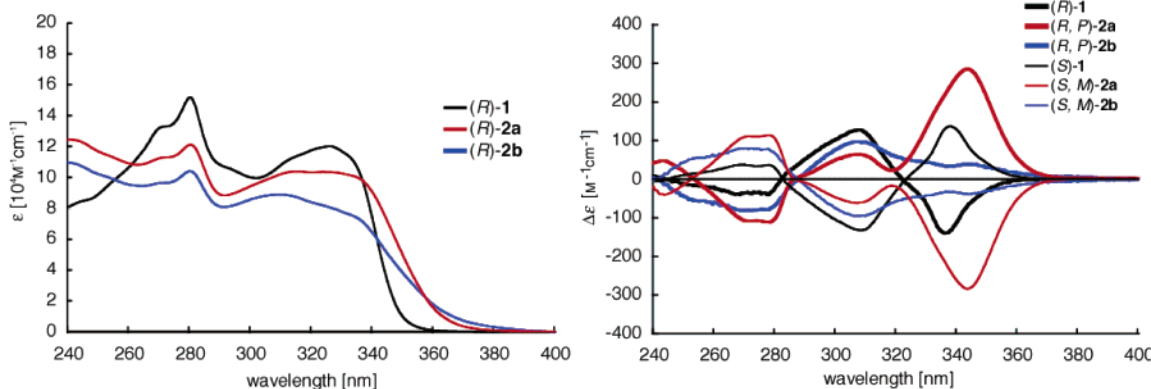


Figure 2. UV/Vis and CD spectra of **1** and **2**: (a, left panel) UV/vis spectra of (*R*)-**1** in CH₂Cl₂, (*R*)-**2a** in 95:5 CHCl₃/DMF, and (*R*)-**2b** in CH₂Cl₂; (b, right panel) CD spectra of (*R*)- and (*S*)-**1** in CH₂Cl₂, (*R,P*)- and (*S,M*)-**2a** in 95:5 CHCl₃/DMF, and (*R*)- and (*S*)-**2b** in CH₂Cl₂.

parent peak, but a peak appeared assignable to the 1:1 species corresponding to 1/Ag⁺ or 1/Cu⁺ in which one of the metal ions and all PF₆ anions had been removed from **2a** and **2b**, probably because of weak coordination bonding and possibly metal–metal repulsion in the multimetal coordination. This nevertheless does not mean that **2a** and **2b** possess a 1:1 composition. The 2:1 stoichiometry is supported by titration experiments in circular dichroic (CD) spectra (vide infra). Furthermore, ¹H NMR spectrum of a 1:1 mixture of **1** and AgPF₆ exhibited only broad signals, in contrast to the sharp signals of **2a**.

While complexes **2a,b** exhibited no significant difference from free **1** in UV–vis spectra, [α]_D values were greatly altered (Scheme 2). The negative value of (*R*)-**1** was converted to large positive values upon complexation, and the reverse transition occurred on complexation of (*S*)-**1**. Since such enormous variation cannot be induced solely by deformation of the binaphthyl core, it is reasonable to conclude that the chirality has emerged from the strands as well. Similar behavior found in the Cozzi–Siegel protocol with oligo(bipyridine ether) strands was attributed to double-helix formation.⁵

Analysis of CD spectra also supported the emergence of chirality in the strands (Figure 2). The strong Cotton effect with a zero point at 320 nm observed for (*R*)- and (*S*)-**1** disappeared in the complexes. Alternatively, the silver complexes exhibited a strong peak at 345 nm and a medium peak at 310 nm, whereas only a broad peak was observed at 310 nm in the copper complexes.¹² Such spectral changes were characteristic of double-helix formation in our previous study on chiral acetylenic cyclophanes.⁶ It is highly probable, therefore, that double helicates are formed in both silver and copper complexes. The completely reversed spectral profiles of the complexes derived from antipodal (*R*)- and (*S*)-**1** imply that the helical modes of strands in these complexes are heterochiral.¹³ The 2:1 metal/1 stoichiometry of the complexes was confirmed on the basis of CD spectra through titration with the metal (Figure 3). Upon increasing the amount of the silver salt added to (*R*)-**1**, the negative-sign band at 340 nm diminished gradually while a new positive-sign band at 345 nm appeared. The intensity of this

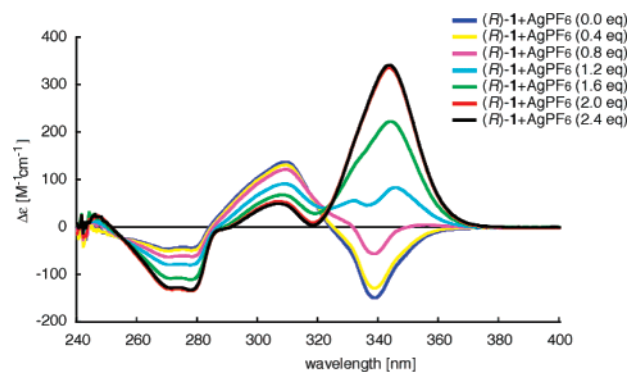


Figure 3. CD spectral changes upon titration of (*R*)-**1** with AgPF₆ in 95:5 CHCl₃/DMF.

band reached an upper limit at the 2:1 metal/1 ratio and experienced no more enhancement beyond this ratio.

Control experiments suggest that these features do not arise from a dimer or higher oligomers. A ligand with a single strand, (*R*)-**3**, that necessarily leads to intermolecular association upon interaction with metals was synthesized (Scheme 3). Treatment of **3** with 1 equiv of AgPF₆ or [(CH₃CN)₄Cu]PF₆ afforded white or yellow precipitates. However, these precipitates exhibited [α]_D values and CD spectra similar to those of free **3**.¹⁴ This suggests either that no effective intermolecular complexation occurred or that the *P*- and *M*-sense helicates were formed in equal amounts even if the complex had been formed in solution providing an unequivocal evidence for *no intermolecular complexation* in **2**. Apparently, the twin strands in **1** are crucial for enantiomerically pure double-helix formation through *intra*-molecular coordination.

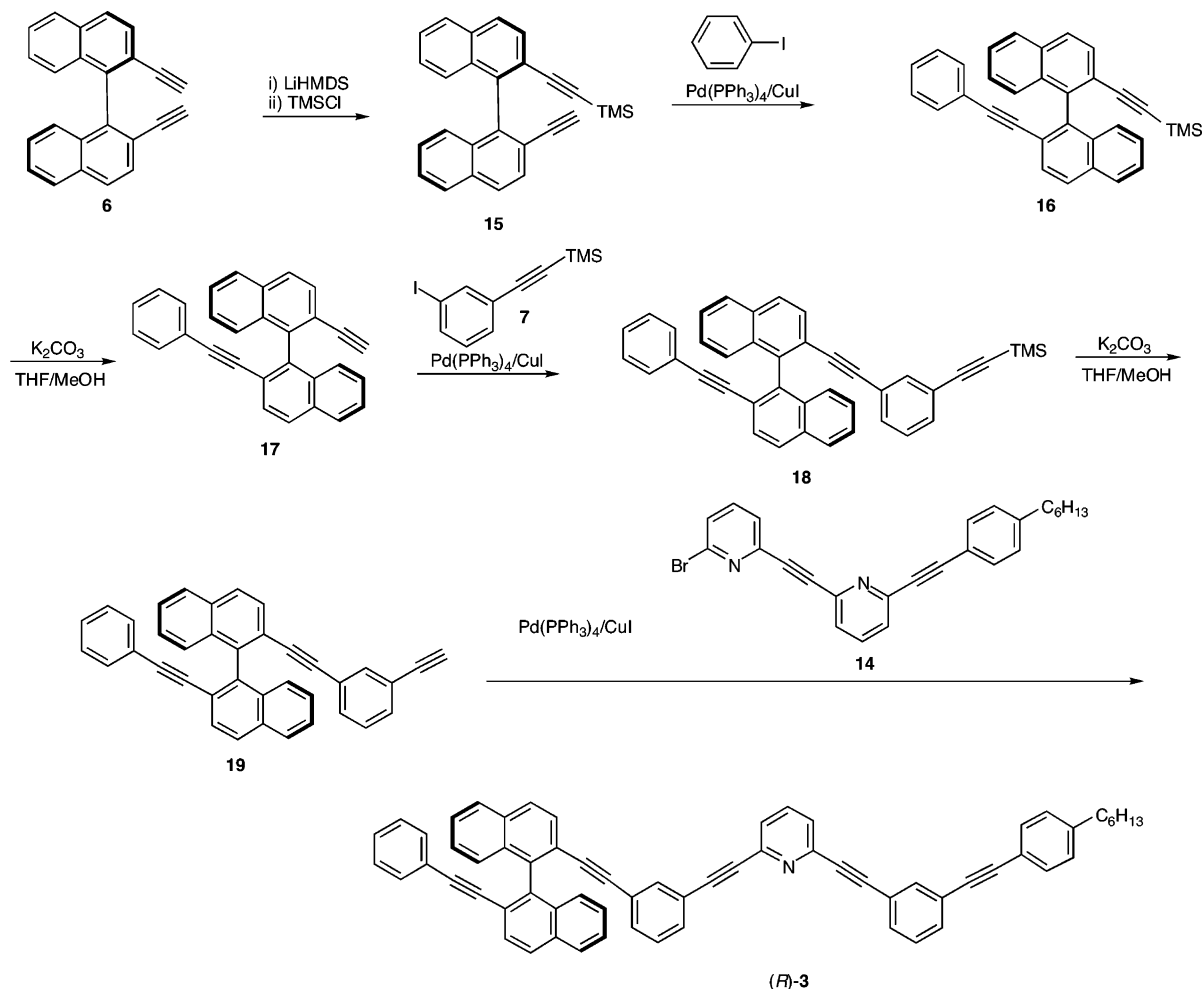
As described above, double-helix formation induces a dramatic variation of CD spectra at around 350 nm. However, this region is covered by a strong band derived from a chromophore associated with the binaphthyl–arylacetylene moiety, as is evident from the spectrum of 2,2′-bis(phenylethynyl)-1,1′-binaphthalene.⁶ To sort out the contribution of the double-helical arylene ethynylene motif, substrates **4** without binaphthyl–acetylene connection were synthesized (Scheme 4). As expected, these compounds were almost transparent above 300 nm in CD spectra (Figure 4). On the other hand, both silver and copper complexes gave rise to characteristic bands in this region, though

(12) A strong band at 323 nm was observed in CD spectra of single-helical phenylene ethynyls: Gin, M. S.; Yokozawa, T.; Prince, R. B.; Moore, J. S. *J. Am. Chem. Soc.* **1999**, *121*, 2643–2644. CD spectra for alternating binaphthylene/diyne units were also reported: Chow, H.-F.; Ng, M.-K. *Tetrahedron: Asymmetry* **1996**, *7*, 2251–2262.

(13) Helical polysilanes exhibited similar bias in CD spectra resulting in positive and negative sign bands from *P*- and *M*-screw-sense backbones, respectively: Fujiki, M. *J. Am. Chem. Soc.* **1994**, *116*, 11976–11981.

(14) [α]_D³¹ values: −74.4 (c 0.50, CH₂Cl₂) for (*R*)-**3**; −93.4 (c 0.50, THF) for (*R*)-**3**/AgPF₆; −56.5 (c 0.53, CH₂Cl₂) for (*R*)-**3**/[(CH₃CN)₄Cu]PF₆. CD spectra are shown in Supporting Information.

Scheme 3



the $\Delta\epsilon$ values are not so large as those observed for the complexes with **1**.

As depicted in Scheme 2, molecular modeling leads to (*R,P*)- and (*S,M*)-conformers for both enantiomers. To confirm the sense of the helicity, we invoked the CD exciton chirality method.¹⁵ A chromophore to be attached should exhibit a Cotton effect at a long wavelength because the compound has conjugated aromatic acetylene moieties. Since an anthryl chromophore has a ¹L_a absorption band in the long-wavelength region, although its intensity is rather weak,¹⁶ we synthesized ligands (*R*)- and (*S*)-**5** according to the procedure shown in Scheme 5. The metal complex of (*R*)-**5** should give rise to the negative exciton chirality, as depicted in Figure 5, and vice versa. The CD spectra of **5** are transparent in the region above 400 nm (Figure 6). On the other hand, the negative exciton chirality was explicitly observed upon interaction of (*R*)-**5** with AgPF₆: a first negative Cotton effect at 485 nm ($\Delta\epsilon = -70$) and a second Cotton effect at 438 nm ($\Delta\epsilon = 41$).¹⁷ The antipodal (*S*)-**5** exhibited a completely reversed feature. The optimized structure

for the Ag(I) complex based on AM1 calculations¹⁸ is shown in Figure 7. Notably, the angle between the transition dipole moments for the ¹L_a absorption band was found to be 86.5°. This is important because no CD exciton coupling arises when the two dipole moments are aligned in parallel or antiparallel. Apparently, the metal complexation causes both ends of the strands to approach each other, and the sense of helicity thus induced is consistent with the prediction on the basis of molecular modeling. The copper complex also exhibited virtually the same chirality although the Cotton effects were detected faintly.

In summary, incorporation of pyridine moieties into the arylene ethynylene strands induced assembly to double helicates. The helicate formation could be unambiguously elucidated by characteristic variations of $[\alpha]_D$ values and CD spectra. The CD exciton chirality method enabled us to assign the sense of helicity, which is consistent with prediction by molecular modeling. Further investigations of this novel class of compounds are in progress in our laboratories.

Experimental Section

Preparation of (*R,P*)-2a. A 10 mL flask was charged with (*R*)-**1** (24.6 mg, 0.020 mmol) and THF (2 mL), and then AgPF₆ (11.1 mg,

(15) (a) Harada, N.; Nakanishi, K. *Circular Dichroic Spectroscopy-Exciton Coupling in Organic Stereochemistry*; University Science Books: Mill Valley, CA, 1983. (b) Nakanishi, K.; Berova, N. In *Circular Dichroism Principles and Applications*; Nakanishi, K., Berova, N., Woody, R. W., Eds; VCH Publishers Inc.: New York, 1994.
 (16) (a) Harada, N.; Takuma, Y.; Uda, H. *J. Am. Chem. Soc.* **1976**, *98*, 5408–5409. (b) Harada, N.; Takuma, Y.; Uda, H. *Bull. Chem. Soc. Jpn.* **1977**, *50*, 2033–2038. (c) Harada, N.; Takuma, Y.; Uda, H. *J. Am. Chem. Soc.* **1977**, *100*, 4029–4036.

(17) A very broad trough of the ¹L_a absorption band was observed for 2,2'-substituted 9,9'-bianthryls: Toyota, S.; Shimasaki, T.; Tanifuji, N.; Wakamatsu, K. *Tetrahedron: Asymmetry* **2003**, *14*, 1623–1629.
 (18) Stewart, J. J. P. MOPAC 2002; Fujitsu Limited: Tokyo, Japan, 2001.

Scheme 4

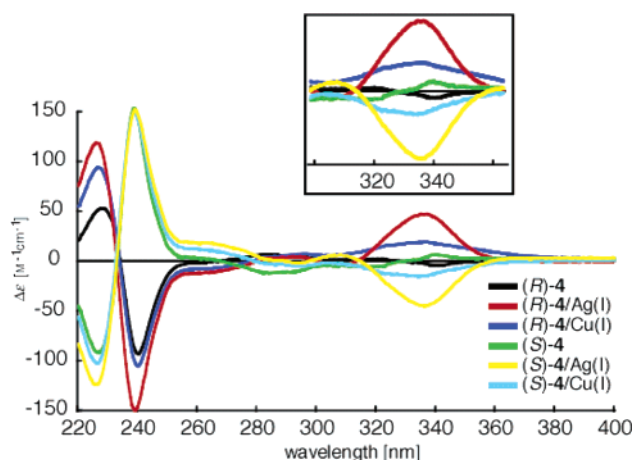
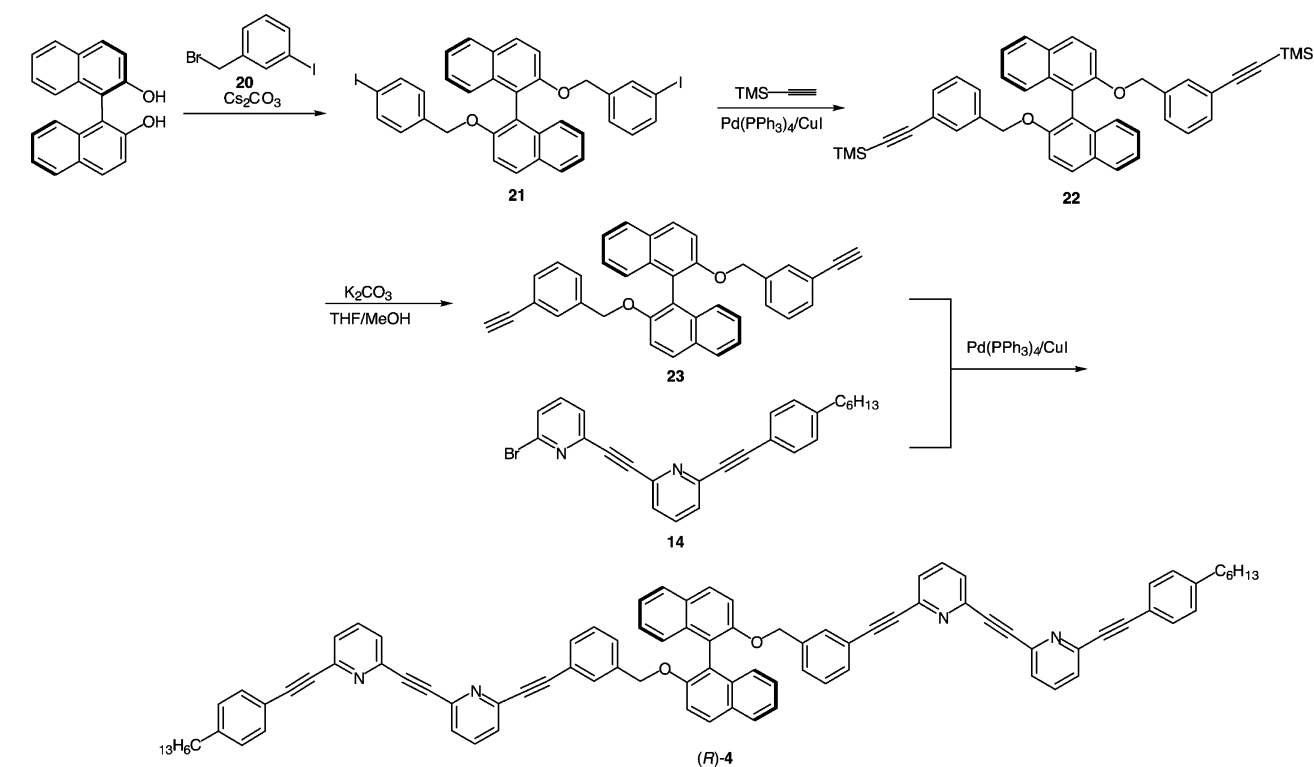


Figure 4. CD spectra of **4** and their metal complexes in THF.

0.044 mmol) in THF (2 mL) was added. After the mixture had been stirred at room temperature for 1 h in the dark, the solvent was evaporated in vacuo. The obtained crude solid was washed repeatedly with THF (2 mL \times 5). After drying in vacuo, the white solid obtained was used for the spectroscopic measurements. $^1\text{H NMR}$ (acetone- d_6) 500 MHz: δ 0.83–0.88 (m, 6H), 1.23–1.30 (m, 12H), 1.54 (t, J = 7.3 Hz, 4H), 2.55 (t, J = 7.0 Hz, 4H), 5.94 (d, J = 7.9 Hz, 2H), 6.87 (t, J = 8.3 Hz, 2H), 7.06 (t, J = 8.2 Hz, 4H), 7.08 (t, J = 8.2 Hz, 4H), 7.20–7.27 (m, 6H), 7.31 (t, J = 7.6 Hz, 4H), 7.35 (s, 2H), 7.50–7.65 (m, 8H), 7.68 (t, J = 7.6 Hz, 2H), 7.77 (t, J = 8.2 Hz, 2H), 7.89 (d, J = 8.2 Hz, 2H), 8.14 (d, J = 7.9 Hz, 2H). $[\alpha]_D^{30.2}$ = +1765.10 (c 0.4, acetone). UV/Vis (5% DMF in CHCl_3 , 8.15×10^{-5} M): λ_{max} (ϵ_{max}) = 228 nm (14.4×10^4), 280 nm (12.5×10^4), 327 nm (10.7×10^4). CD (c 8.15×10^{-5} M in 5% DMF in CHCl_3 , 0.1 cm cell): θ = 1.3, $\Delta\epsilon$ = 47.6 (at 243 nm); θ = -3.0, $\Delta\epsilon$ = -111.5 (at 279 nm); θ = 1.7, $\Delta\epsilon$ = 64.3 (at 307 nm); θ = 0.6, $\Delta\epsilon$ = 22.5 (at 319 nm); θ = 7.7, $\Delta\epsilon$ = 285.7 (at 344 nm). Enantiomer (*S,M*)-**2a** was prepared from (*S*)-**1** analogously. (*S,M*)-**2a**: $[\alpha]_D^{30.2}$ = -1742.82 (c 0.5, acetone). UV/Vis

(5% DMF in CHCl_3 , 8.15×10^{-5} M): λ_{max} (ϵ_{max}) = 228 nm (13.9×10^4), 281 nm (11.9×10^4), 325 nm (10.3×10^4). CD (c 8.15×10^{-5} M in 5% DMF in CHCl_3 , 0.1 cm cell): θ = -1.1, $\Delta\epsilon$ = -40.6 (at 244 nm); θ = 3.1, $\Delta\epsilon$ = 113.6 (at 278 nm); θ = -1.7, $\Delta\epsilon$ = -61.9 (at 307 nm); θ = -0.5, $\Delta\epsilon$ = -16.9 (at 319 nm); θ = -7.6, $\Delta\epsilon$ = -284.3 (at 344 nm).

Preparation of (*R,P*)-2b**.** A 10 mL flask was charged with (*R*)-**1** (24.6 mg, 0.020 mmol) and dichloromethane (2 mL), and then $[\text{Cu}(\text{MeCN})_4]\text{PF}_6$ (16.4 mg, 0.044 mmol) in dichloromethane (2 mL) was added. After the mixture had been stirred at room temperature for 3 h, the solvent was evaporated in vacuo. The yellow solid obtained was used for the spectroscopic measurements. (*R,P*)-**2b**: $[\alpha]_D^{30.1}$ = +623.74 (c 0.4, CH_2Cl_2). UV/Vis (CH_2Cl_2 , 8.15×10^{-5} M): λ_{max} (ϵ_{max}) = 218 nm (10.8×10^4), 280 nm (9.0×10^4), 309 nm (9.1×10^4). CD (c 8.15×10^{-5} M in CH_2Cl_2 , 0.1 cm cell): θ = 0.3, $\Delta\epsilon$ = -9.2 (at 230 nm); θ = -0.3, $\Delta\epsilon$ = -9.5 (at 237 nm); θ = 2.2, $\Delta\epsilon$ = -80.2 (at 269 nm); θ = -2.6, $\Delta\epsilon$ = -95.7 (at 308 nm); θ = -1.1, $\Delta\epsilon$ = -39.3 (at 344 nm).

Silver and copper complexes of (*R*)-**3** were prepared by the analogous procedure for **2a** and **2b**. (*R*)-**3**/AgPF₆ complex: a white foam, $[\alpha]_D^{31.1}$ = -93.39 (c 0.500, THF). UV/Vis (THF, 1.1×10^{-4} M): λ_{max} (ϵ_{max}) = 223 nm (6.0×10^4), 279 nm (8.8×10^4), 327 nm (5.9×10^4). CD (c 1.1×10^{-4} M in THF, 0.1 cm cell): θ = -1.1, $\Delta\epsilon$ = -36.7 (at 230 nm); θ = 0.3, $\Delta\epsilon$ = 9.4 (at 241 nm); θ = -1.3, $\Delta\epsilon$ = -31.1 (at 276 nm); θ = 3.9, $\Delta\epsilon$ = 107.7 (at 307 nm); θ = -3.4, $\Delta\epsilon$ = -93.1 (at 335 nm). (*R*)-**3**/[Cu(MeCN)₄]PF₆ complex: a yellow solid, $[\alpha]_D^{31.1}$ = (c -56.51, CH_2Cl_2). UV/Vis (CH_2Cl_2 , 8.82×10^{-5} M): λ_{max} (ϵ_{max}) = 220 nm (8.1×10^4), 279 nm (8.7×10^4), 310 nm (8.1×10^4). CD (c 8.82×10^{-5} M in CH_2Cl_2 , 0.1 cm cell): θ = -0.9, $\Delta\epsilon$ = -30.7 (at 230 nm); θ = 0.3, $\Delta\epsilon$ = 9.5 (at 242 nm); θ = -0.7, $\Delta\epsilon$ = -26.5 (at 276 nm); θ = 3.0, $\Delta\epsilon$ = 101.7 (at 307 nm); θ = -2.0, $\Delta\epsilon$ = -70.1 (at 335 nm).

Silver and copper complexes of **4** were prepared by the analogous procedure for **2a** and **2b**. (*R*)-**4**/AgPF₆ complex: a white foam, $[\alpha]_D^{30.7}$ = -186.37 (c 1.000, THF). UV/Vis (THF, 6.4×10^{-5} M): λ_{max} (ϵ_{max}) = 237 nm (15.7×10^4), 298 nm (6.4×10^4), 327 nm (6.6×10^4). CD (c 6.4×10^{-5} M in THF, 0.1 cm cell): θ = -0.2, $\Delta\epsilon$ = -7.2 (at 217

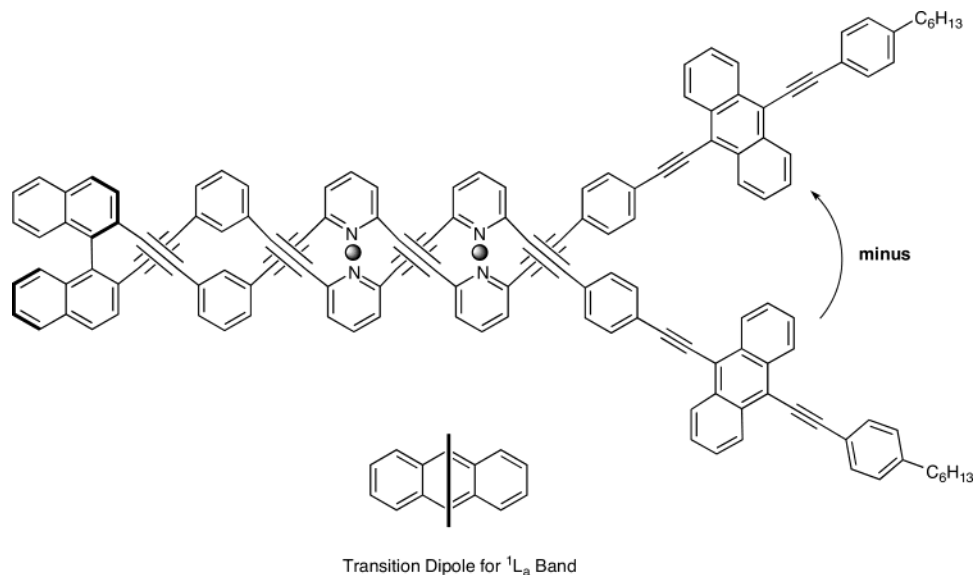


Figure 5. Correlation between the structure of metal complex of (*R*)-**5** and the negative CD exciton chirality.

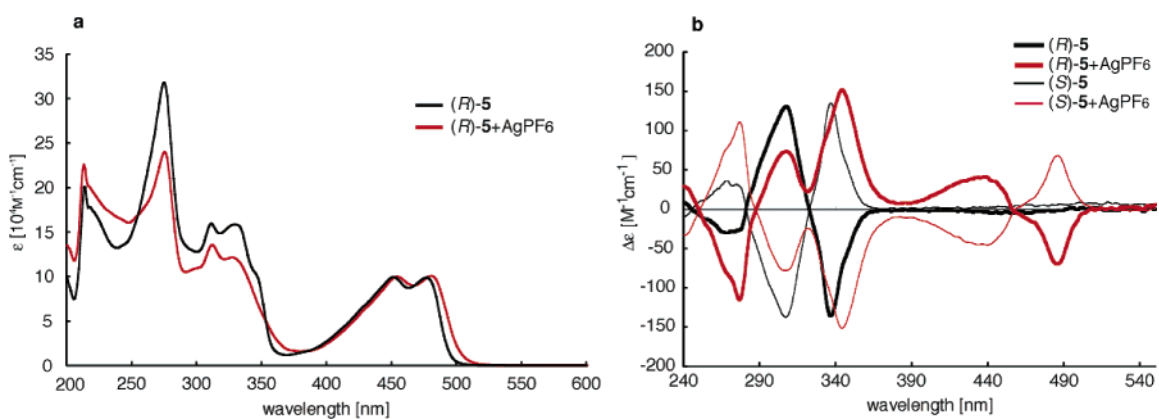
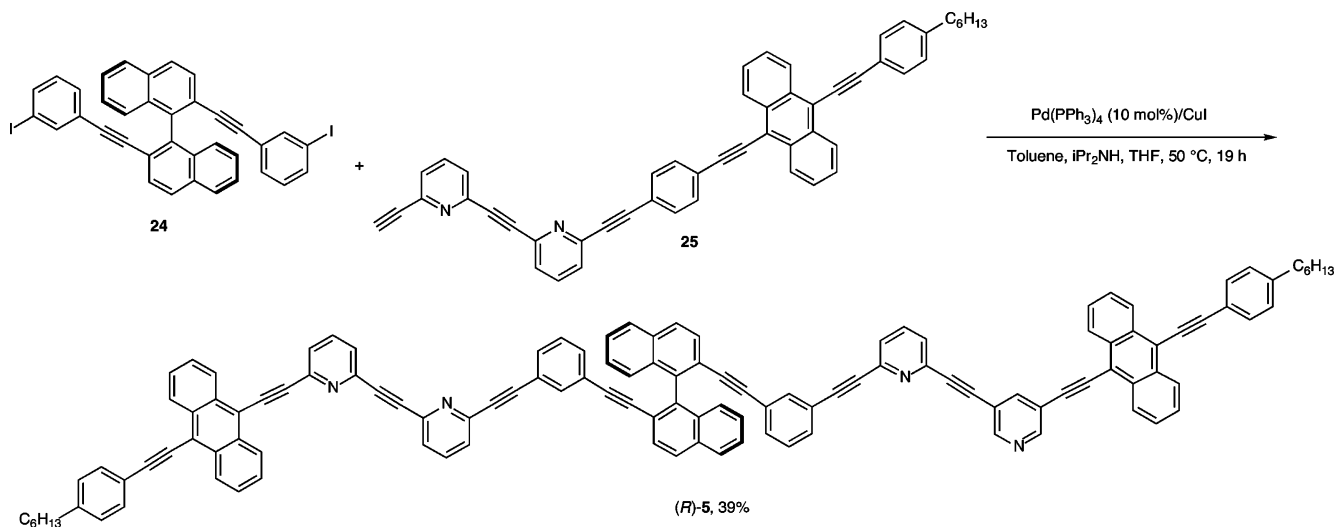


Figure 6. UV/Vis and CD spectra of **5** and their Ag^+ complexes: (a) UV/vis spectra of (*R*)-**5** and its AgPF_6 complex in THF; (b) CD spectra of (*R*)- and (*S*)-**5** and their AgPF_6 complexes in THF.

Scheme 5



nm); $\theta = 1.8$, $\Delta\epsilon = 88.0$ (at 234 nm); $\theta = -2.3$, $\Delta\epsilon = -110.9$ (at 250 nm); $\theta = 0.4$, $\Delta\epsilon = 19.0$ (at 287 nm); $\theta = 0.1$, $\Delta\epsilon = 4.7$ (at 306 nm); $\theta = 0.9$, $\Delta\epsilon = 42.2$ (at 329 nm). (*S*)-**4**/ AgPF_6 complex: $[\alpha]_D^{28.6} = -176.20$ (*c* 0.500, THF). UV/Vis (THF, 8.1×10^{-5} M): λ_{max} (ϵ_{max}) = 231 nm (18.8×10^4), 297 nm (5.7×10^4), 325 nm (6.2×10^4). CD (*c*

8.1×10^{-5} M in THF, 0.1 cm cell): $\theta = -3.3$, $\Delta\epsilon = -124.0$ (at 227 nm); $\theta = 4.1$, $\Delta\epsilon = 151.9$ (at 239 nm); $\theta = -0.1$, $\Delta\epsilon = -2.2$ (at 294 nm); $\theta = 0.2$, $\Delta\epsilon = 6.3$ (at 308 nm); $\theta = -1.2$, $\Delta\epsilon = -44.9$ (at 337 nm). (*R*)-**4**/ $[\text{Cu}(\text{MeCN})_4]\text{PF}_6$ complex: a yellow solid, $[\alpha]_D^{37.5} = +202.95$ (*c* 0.400, THF). UV/Vis (THF, 6.6×10^{-5} M): λ_{max} (ϵ_{max}) =

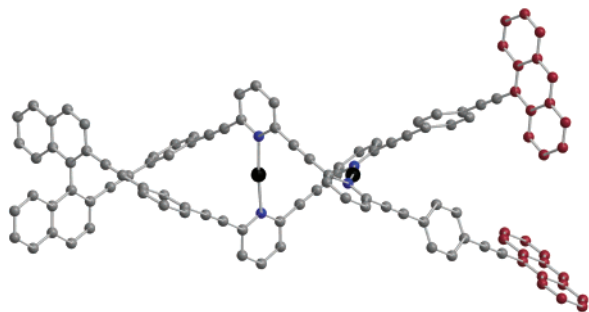


Figure 7. Structure of (R)-5/2Ag⁺ optimized by AM1 calculations.

232 nm (14.1×10^4), 296 nm (5.4×10^4), 339 nm (4.2×10^4). CD (c 6.6×10^{-5} M in THF, 0.1 cm cell): $\theta = 2.0$, $\Delta\epsilon = 94.2$ (at 227 nm); $\theta = -2.3$, $\Delta\epsilon = -105.6$ (at 240 nm); $\theta = 0.4$, $\Delta\epsilon = 19.1$ (at 336 nm). (S)-4/[Cu(MeCN)₄]PF₆ complex: $[\alpha]_D^{29.2} = -200.68$ (c 0.500, THF). UV/Vis (THF, 8.1×10^{-5} M): λ_{\max} (ϵ_{\max}) = 232 nm (16.1×10^4), 284 nm (5.8×10^4), 322 nm (5.1×10^4). CD (c 8.1×10^{-5} M in THF, 0.1 cm cell): $\theta = -2.8$, $\Delta\epsilon = -103.1$ (at 227 nm); $\theta = 4.1$, $\Delta\epsilon = 149.2$ (at 239 nm); $\theta = -0.1$, $\Delta\epsilon = -15.5$ (at 335 nm).

Preparation of (R)-5/AgPF₆ Complex. A 10 mL flask was charged with (R)-1 (12.0 mg, 0.0066 mmol) and THF (2 mL), and then AgPF₆ (3.8 mg, 0.015 mmol) in THF (0.4 mL) was added. After the mixture had been stirred at room temperature for 1.5 h in the dark, the solvent was evaporated in vacuo. The orange solid obtained was used for the CD measurements. (R)-5/AgPF₆: $[\alpha]_D^{22.6} = +445.51$ (c 0.068, CH₂-Cl₂). UV/Vis (CH₂Cl₂, 5.58×10^{-5} M): λ_{\max} (ϵ_{\max}) = 218 nm ($2.3 \times$

10^5), 277 nm (2.6×10^5), 313 nm (1.5×10^5), 458 nm (1.0×10^5), 483 nm (1.1×10^5). CD (THF, 5.58×10^{-5} M, 0.1 cm cell): $\theta = 5.4$, $\Delta\epsilon = 29.6$ (at 239 nm); $\theta = -21.3$, $\Delta\epsilon = -115.6$ (at 276.5 nm); $\theta = 13.5$, $\Delta\epsilon = 73.4$ (at 307 nm); $\theta = 4.1$, $\Delta\epsilon = 22.3$ (at 322 nm); $\theta = 27.9$, $\Delta\epsilon = 151.5$ (at 344.5 nm); $\theta = 1.2$, $\Delta\epsilon = 6.6$ (at 381 nm); $\theta = 7.6$, $\Delta\epsilon = 41.2$ (at 438 nm); $\theta = -12.9$, $\Delta\epsilon = -70.1$ (at 485.5 nm). Enantiomer (S)-5/AgPF₆ was prepared from (S)-5 analogously. (S)-5/AgPF₆: CD (THF, 5.99×10^{-5} M, 0.1 cm cell): $\theta = 21.9$, $\Delta\epsilon = 110.8$ (at 276.5 nm); $\theta = -15.4$, $\Delta\epsilon = -78.2$ (at 307.5 nm); $\theta = -4.8$, $\Delta\epsilon = -24.2$ (at 321.5 nm); $\theta = -30.0$, $\Delta\epsilon = -151.8$ (at 344 nm); $\theta = -2.0$, $\Delta\epsilon = -10.1$ (at 382.5 nm); $\theta = -9.0$, $\Delta\epsilon = -45.8$ (at 439.5 nm); $\theta = 13.4$, $\Delta\epsilon = -67.9$ (at 486 nm).

The experimental details for arylene ethynylene ligands are given in Supporting Information.

Acknowledgment. We thank M. Yasui and H. Mitsuta for their technical assistance. Financial support from New Energy and Industrial Technology Development Organization (NEDO) of Japan for Industrial Technology Research Grant Program (01B68006d) and the Sumitomo Foundation to A.O. is gratefully acknowledged.

Supporting Information Available: Syntheses and spectroscopic characterizations of **1**, **3–5**, **9**, **11–19**, **21–23**, and **25** (PDF). This material is available free of charge via the Internet at <http://pubs.acs.org>.

JA048327D